Spatial Heterogeneity of Viral Suppression and Viral Rebound Patterns among ART Patients in Zimbabwe from 2004 to 2017: A Bayesian Mixed Effects Multistate Model

Zvifadzo Matsena Zingoni[1,2,*], Tobias F. Chirwa[1], Jim Todd[3] and Eustasius Musenge[1]

[1]*Division of Epidemiology and Biostatistics, School of Public Health, Faculty of Health Sciences, University of the Witwatersrand, Johannesburg, South Africa*

[2]*Ministry of Health and Child Care, National Institute of Health Research, Causeway, Harare, Zimbabwe*

[3]*Department of Population Health, London School of Hygiene and Tropical Medicine, London, United Kingdom*

Abstract: Augmenting the global efforts towards HIV control and prevention, spatial modelling helps identify areas with poor viral suppression to inform programme planning. This study aims to describe the spatial viral suppression and viral rebound trajectories among ART patients. This is the first application of the fully Bayesian geoadditive semiparametric multistate Markov models to account for unobserved geographical heterogeneity. Time-varying log-baseline effects of the transition intensities and non-linear effects of continuous covariates were estimated as smoothed functions of time using penalised splines. Non-parametric effects of fixed covariates and frailty effects to account for individual variability were also considered. Viral load was the preferred marker for better prediction of HIV/AIDS disease progression; therefore, a three staged model was proposed bases on two viral load transient states defined by undetectable viral cut-off limits and death as the third absorbing state. Model application was based on the routinely collected individual-level data of ART patients from the Zimbabwe national ART programme. Amongst 18,150 participants, both the log-baseline transition rates of attaining undetectable viral suppression and attaining a viral rebound increased with increase in ART duration. Viral rebound transition was significantly prevalent among patients living on the long-distance truck route region (Matabeleland North province) which borders with Botswana and Zambia. Interventions which address health literacy and misconceptions over ART benefits and the gravity of attaining and sustaining viral suppression are a priority in the fight of HIV to increase patients' life expectancy and lower HIV transmission.

Keywords: Bayesian estimation, multistate Markov models, spatial heterogeneity, viral suppression, viral rebound.

1. INTRODUCTION

Multistate models are useful in the management of chronic diseases since intermediate transitions give quick insights into the complex pathways patients experience before the final event, death, occurs [1]. Regarding Human immune-deficiency virus (HIV) infections, multistate models can be used to evaluate the performance of antiretroviral therapy (ART) programmes and identify patients who are at a high risk of immune deterioration so that appropriate interventions can be implemented.

Numerous studies assessing HIV disease progression using multistate models have used the frequentist estimation approach implemented in R using the *msm* package [2]; however, these frequentist multistate models have some limitations. Firstly, they are unable to account for unexplained individual heterogeneity in transition rates which may be represented by the random-effects model. Accounting for individual variation is crucial in infectious disease modelling since individuals respond differently to treatment [2]. Secondly, frequentist multistate models are restrictive on the types of covariates they can handle, as the functional form of the effects of the predictive factors is assumed to be linear (or log-linear). As a result, the effects of the covariates may be poorly estimated and penalized-splines (P-splines) may better estimate non-linear functions for these covariates. Such errors in covariate misspecification may lead to inaccurate statistical conclusions, increased bias in estimates and decreased statistical power for statistical significance tests [2]. Besides, most of the previous studies focusing on HIV disease progression have used CD4 cell count measurements to define the finite number of states which is known to have measurement error; hence, may not be sensitive enough to assess HIV disease progression [3]. In line with the global recommendation to use viral load in HIV monitoring, a recent study confirmed the superiority of viral load measurements in predicting ART outcomes compared to CD4 cell counts [4].

The work by Kneib and Hennerfeind (2008) [5] on the use of Bayesian inference in multistate models forms the basis of this study analysis [5]. In this model,

Address correspondence to this article at the Division of Epidemiology and Biostatistics, School of Public Health, Faculty of Health Sciences, University of the Witwatersrand, 27 St Andrew's, Parktown, Postal code 2193, Johannesburg, South Africa; E-mail: zmatsena28@gmail.com

E-ISSN: 1929-6029/19

the transition (hazard) rates are estimated in a multiplicative Cox-type way whereby the nonparametric effects of the log-baseline hazard are simultaneously estimated with other predictor components and assumed to be time-varying. The flexible linear predictor of the model can handle non-linear effects of continuous covariates modelled using P-splines [6]. Additional components may include covariates with time-varying effects; non-linear effects of a continuous covariate modelled non-parametrically with a smoothing function; parametric fixed effects and frailty terms [5]. However, to our knowledge, no studies have included the spatial random effects in the flexible predictor using multistate models; hence, this current study aims to incorporate the spatial covariate in a multistate model framework which is crucial to account for unobserved heterogeneity. Despite the recent emerging of spatial modelling in HIV monitoring indicators [7], there has not been extensive use of spatial data on time-varying viral suppression and time-varying viral rebound indicators to monitor HIV disease progression among ART patients.

The World Health Organization (WHO) HIV monitoring guidelines recommend the use of viral load which also became one of the indicators in the UNAIDS 90-90-90 fast track targets whereby 90% of all people living with HIV (PLWHIV) know their status, 90% of those who know their status receive ART and 90% of those on ART achieve viral suppression [8]. In Zimbabwe, only 73% of ART patients were estimated to be virally suppressed in 2018, which is a concern for HIV prevention and control in the country [9]. With the global quest to achieve zero new HIV infections by 2030, the focus is on attaining an undetectable viral load among HIV-infected population since undetectable HIV results in un-transmittable virus (U=U) [10]. The use of viral load monitoring in HIV disease progression is important to enhance understanding of HIV infection to the various stakeholders and provides a motivation on the need of encouraging ART adherence. Therefore, it is imperative to understand the viral suppression and viral rebound (HIV disease progression) patterns among ART patients. With the scarce resources in low-middle income countries like Zimbabwe, it was also of interest to be able to link these transition trajectories to the geographical regions to pinpoint high burdened areas so as to guide resource allocation and to inform policy on targeted interventions; hence, the inclusion of the spatial frailty term.

This manuscript aimed to describe the spatial heterogeneity of viral suppression to undetectable levels and viral rebound to detectable levels trajectories among ART patients using the Bayesian semi-parametric geoadditive multistate model. The model was fitted on patient-level data from the Zimbabwe national ART programme for patients who initiated ART between 2004 and 2017. In addition to the non-linear continuous covariates, the model accounted for time-varying transition rates and individual heterogeneity which reflects the reality. The spatial component assumed that the viral load transitions were likely to be induced characteristics of geographical units, which may depend on neighboring regions but may as well be heterogenic. We hypothesized that there is spatial heterogeneity of viral suppression and rebound in this cohort and these transition rates change with time. Findings from this study may provide additional information on HIV disease progression and give a proxy on how well the ART patients are adhering to ART so as to achieve un-transmittable virus levels. The knowledge gained from this analysis may also be used to encourage HIV patients to understand the importance of ART adherence.

Data management and preliminary analyses were handled in Stata Statistical Software Version 15.1 [11]. Inference procedures were implemented in free BayesX software package Version 3.0.2 [12] using Markov Chain Monte Carlo (MCMC) simulation technique. Results visualization was performed in RStudio [13]. The rest of the paper is structured as follows: **Section 2** describes the fully Bayesian multistate model formulation (likelihood, prior, posterior), MCMC inference, model validation and diagnostics; **Section 3**, we apply the proposed model to the Zimbabwe national ART program data collected over 13 years; and **Section 4,** we discuss the advantages of these models and highlight the Public Health and statistical implications of our findings. The Supplementary material provides additional detail to Section 2 in addition to the BayesX code used.

2. BAYESIAN GEOADDITIVE MULTISTATE MODEL

2.1. Description of the Multistate Model

In this study, we considered a time-continuous Markov process $\{X(t), t \geq 0\}$ with two reversible transient states and one absorbing (death) state defining the finite states $(S = 1,2,3)$ as depicted in Figure **1**. The viral load cutoff points were based on guidelines for undetectable viral load [10], that is, "undetectable viral suppression (<50copies/mL)" state as state 1, "detectable viral rebound (≥50copies/mL)"

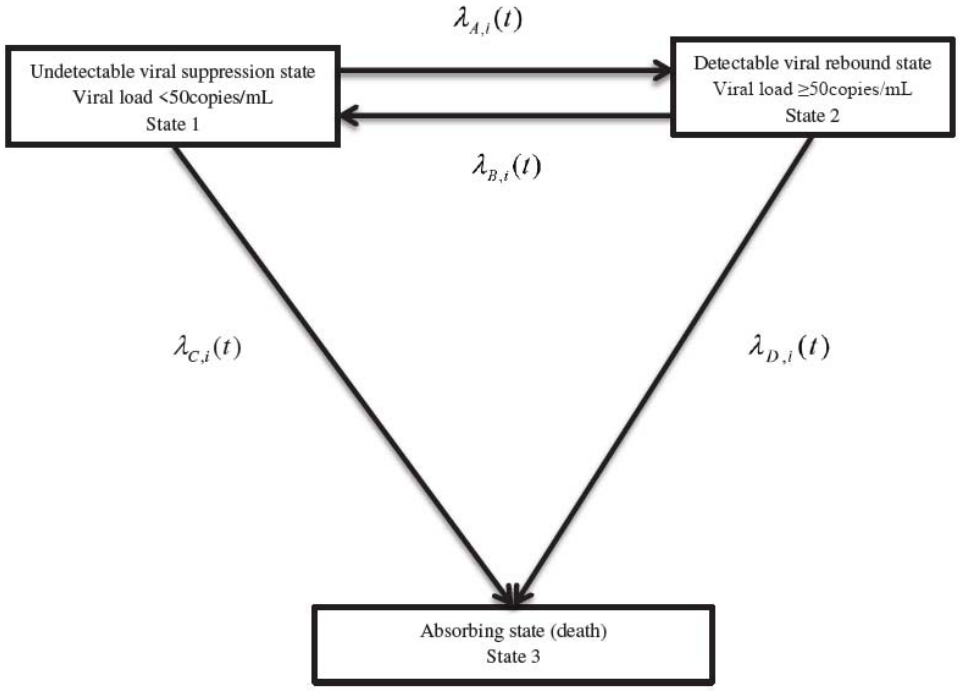

Figure 1: The schematic presentation of HIV disease progression stages multistate model and the corresponding individual-specific transition intensities.

state as state 2 and the absorbing state, death, as state 3.

The multistate model is described by a group of individual-specific hazard rates $\lambda_{jk,i}(t)$ where jk, $(j=1,2,...,J \text{ and } k=1,2,...,K)$, indexes the type of transition from state j to k and $i=1,2,3,...,n$ indexes the individuals. These hazard rates are specified in analogy to hazard rates for continuous-time survival analysis (Appendix 1-4) in a multiplicative semi-parametric regression model way:

$$\lambda_{jk,i}(t)=\exp\left(\eta_{jk,i}(t)\right) \quad (1)$$

where $\eta_{jk,i}(t)$ is an flexible additive predictor expressed as

$$\eta_{jk,i}(t)=g_{jk,0}(t)+\sum_{r=1}^{L} g_{jk,r}(t)u_{r,i}(t)+\sum_{r=1}^{R} f_{jk,r}(t)x_{r,i}(t) + \boldsymbol{v}_i(t)'\boldsymbol{\gamma}_{jk}+f_{jk,spat}(t)(s_i)+b_{jk,i} \quad (2)$$

This flexible predictor's components are defined as:

i. A time-varying, nonparametric baseline effect $g_{jk,0}(t)$ mutual for all observations. Generally, in the conventional Cox approach, the baseline hazard $\lambda_{jk,0}(t)$ remained unspecified; however, in this model, the baseline hazard is reparameterised through $g_{jk,0}(t)=\log\left(\lambda_{jk,0}(t)\right)$ function (Appendix A3). Instead of modelling the hazard rates through a piecewise exponential model assuming that all time depended values are piecewise constant [14], this study estimated the non-linear shape of the log-baseline effect by a P-spline prior of arbitrary degree with a second-order penalty [15].

ii. Covariates $u_{r,i}(t)$ with time-varying effects $g_{jk,r}(t)$. However, in this study, covariates with time-varying effects were not included in the model since no time-varying covariates were included in the received dataset.

iii. Non-linear effects $f_{jk,r}(t)x_{r,i}(t)$ of a continuous covariate $x_{r,i}(t)$. In this study, we considered individual age in years as a continuous covariate modelled non-parametrically with a smoothing function $f_{jk,r}(t)$ as it is directly proportional to time. Similarly, these non-linear effects were modelled by the P-spline prior.

iv. Parametric fixed effects γ_{jk} of covariates $v_i(t)$. The vector of the regression coefficients $\boldsymbol{\gamma}_{jk,c}$ contains the usual linear effects of the vector of fixed effects $\boldsymbol{v}_i(t)$ which were WHO clinical stages (I/II or III/IV) and gender (male or female) in this study.

v. The spatial structural effects $f_{jk,spat}(t)(s_i)$ which form the unique part of our multistate model, where $s = 1,2,...,S$ is a spatial index, with $s_i = S$ if individual i is from region or site s to account for spatial heterogeneity assuming a Gaussian Markov random field (GMRF) prior. The spatial effects in this study where split into two components, that is, $f_{jk,spat}(t)(s_i) = f_{jk,str}(t)(s_i) + f_{jk,unstr}(t)(s_i)$ where $f_{jk,str}(t)(s_i)$ defines the structured (correlated) part and $f_{jk,unstr}(t)(s_i)$ defines the unstructured (uncorrelated) part.

vi. Random effects (frailty) term $b_{jk,i}$ was included to account for individual-specific unobserved heterogeneity.

Additional information on model components is provided in Appendix 5.

To estimate viral suppression, viral rebound and mortality transition rates; and determine the associated spatial heterogeneity of these transitions, the model in Figure **1** assumed that: a patient initiated on potent and effective ART treatment may become virally suppressed to undetectable virus levels, may have detectable viral rebound due to poor adherence or treatment failure, ART defaulting or treatment failure; or may die from any of the states. Baseline characteristics effects (WHO clinical stage at ART initiation and gender) were adjusted for in addition to the spatial and individual frailty terms. Therefore, the four transitions estimated were:

$$\begin{aligned}
\lambda_{A,i}(t) &= \exp\begin{pmatrix}\eta_{A,i}(t) = g_{A,0}(t) + f_A age_i(t) + \gamma_{A,1}(WHOstage)\\ +\gamma_{A,2}(sex) + f_{A,spat}(t)(province_i) + b_{A,i}\end{pmatrix}\\
\lambda_{B,i}(t) &= \exp\begin{pmatrix}\eta_{B,i}(t) = g_{B,0}(t) + f_B age_i(t) + \gamma_{B,1}(WHOstage) + \gamma_{B,2}(sex)\\ +f_{C,spat}(t)(province_i) + b_{B,i}\end{pmatrix}\\
\lambda_{C,i}(t) &= \exp\begin{pmatrix}\eta_{C,i}(t) = g_{C,0}(t) + f_C age_i(t) + \gamma_{C,1}(WHOstage) + \gamma_{C,2}(sex)\\ +f_{C,spat}(t)(province_i) + b_{C,i}\end{pmatrix}\\
\lambda_{D,i}(t) &= \exp\begin{pmatrix}\eta_{D,i}(t) = g_{D,0}(t) + f_D age_i(t) + \gamma_{D,1}(WHOstage) + \gamma_{D,2}(sex)\\ +f_{D,spat}(t)(province_i) + b_{D,i}\end{pmatrix}
\end{aligned} \quad (3)$$

where A defines the viral rebound transition, B defines the undetectable viral suppression transition, C and D defines the mortality transition from undetectable virally suppressed and viral rebound states, respectively.

2.2. The Likelihood Function

The likelihood contribution in a multistate model for each individual $i = 1,2,3,...,n$ is derived from a counting process $N_{jk,i}(t)$, counting j to k transitions for individual i. If we consider $S_{iz}, z = 1,2,...,m_i$ as the individual transition times corresponding to a transition process under the non-informative censoring, the intensity process of the counting process is defined as $\alpha_{jk,i} = I_{jk,i}(t)\lambda_{jk,i}(t)$ where $I_{jk,i}(t)$ is the predictable at risk indicator process and the hazard rate $\lambda_{jk,i}(t)$ defined as in Equation (1). Therefore, the individual log-likelihood function is given by:

$$\log L_i(\boldsymbol{\gamma}, \boldsymbol{\beta}, \boldsymbol{\tau}^2) = \sum_{jk=1}^{JK}\left[\int_0^{Si,m_i} \log\left(\lambda_{jk,i}(t)\, dN_{jk,i}(t) - \int_0^{Si,m_i} \lambda_{jk,i}(t) I_{jk,i}(t)\, dt\right)\right] \quad (4)$$

where $\boldsymbol{\gamma} = \left(\gamma'_{jk,1}, \gamma'_{jk,2}, ..., \gamma'_{jk,d}\right)'$ for $c = 1,2,...,d$ is a vector of all fixed effects parameters, $\boldsymbol{\beta} = \left(\boldsymbol{\beta}_{jk,1}, \boldsymbol{\beta}_{jk,2}, ..., \boldsymbol{\beta}_{jk,p}\right)'$ is a vector of (regression) coefficients, $\boldsymbol{\tau}^2 = \left(\tau^2_{jk,1}, \tau^2_{jk,2}, ..., \tau^2_{jk,y}\right)'$ for $q = 1,2,...,y$ is a vector of all variance components under consideration and S_{i,m_i} denotes the time until an individual i has been observed. In survival models, the first term can be viewed as the log-hazard for uncensored data while the second term reflects the cumulative intensities.

Alternatively, the likelihood can be defined in terms of each individual contributions defined in terms of transition censoring indicators $\delta_{jk,i}(t)$ which is equal to one if a jk transition occurs before time (t) and zero otherwise and the observed transition times $S_{iz}, z = 0,1,...,m_i$ defined by the time an individual experience the transition. The alternative log-likelihood formula is given by:

$$\log L_i(\boldsymbol{\beta}, \boldsymbol{\gamma}, \boldsymbol{\tau}^2) = \sum_{z=1}^{m}\sum_{j,k=1}^{JK}\left[\delta_{jk,i}(S_{iz})\log\left(\lambda_{jk,i}(S_{iz})\right) - I_{jk,i}(S_{iz})\int_{S_{i,z=1}}^{S_{iz}} \lambda_{jk,i}(t)\, dt\right] \quad (5)$$

where $\lambda_{jk,i}(t)$ is defined by Equation (1) and this whole expression reflects the commonly known hazard rate models fitted for continuous survival times. If the degree of the P-spline prior for the log-baseline hazard function is greater than one, then the likelihood integral can no longer be solved in a closed form. Detailed steps of the log-likelihood are provided in Appendix 6.

2.3. The Prior Specifications

We performed a fully Bayesian inference since all unknown parameters were assigned prior information.

We assigned non-informative diffuse prior, $P(\gamma) \propto const$ to the *fixed-effects parameters*; alternatively, a weak (large variance) normal prior can be used. The *individual random effects* $b_{jk,i}$ were assumed to be independent and identically distributed (iid) Gaussian distributed with a transition specific precision, $b_{jk,i} \sim N(0, \tau^2_{jk,b})$. Priors for the *random effects (regression) coefficients parameter* vector $\boldsymbol{\beta}_{jk,r}$ for $r = 0,1,...,p$ were assumed to be Gaussian distributed computed as a product of conditional densities defined by the random walk smoothness priors. The general form of the prior for $\boldsymbol{\beta}_{jk,r}$ is given by:

$$P\left(\boldsymbol{\beta}_{jk,r} / \tau^2_{jk,r}\right) \propto \exp\left(-\frac{\boldsymbol{\beta}'_{jk,r}\boldsymbol{W}_{jk,r}\boldsymbol{\beta}_{jk,r}}{2\boldsymbol{\tau}^2_{jk,r}}\right) \quad (6)$$

where $\boldsymbol{W}_{jk,r} \geq 0$ is a precision or penalty matrix of rank $(\boldsymbol{W}_{jk,r}) = h_{jk,r}$. The variance $\tau^2_{jk,r}$ acts as an inverse smoothness hyper-parameter controlling for the trade-off between smoothness and flexibility. That is a small value of $\tau^2_{jk,r}$ corresponds to an increase of the penalty or shrinkage (error) or vice-versa.

Unknown *nonparametric effects* $f_{jk,r}(t)$ of continuous smooth covariate x_r were estimated using Bayesian P-splines [6] as a linear combination of a larger number of B-splines basic functions B_d, i.e., $f_{jk,r}(x_r) = \sum_{d-1}^{D_r} \boldsymbol{\beta}_{jk,rd} B_d(x_r)$. The basic functions B_d are the B-splines of a known degree l on a set of equally spaced knots $x_r(\max) = \varsigma_0 < \varsigma_1 < \varsigma_2 < ... < \varsigma_{s-1} < \varsigma_s = x_r(\max)$ within the main domain of x_r, $D_r = l + s$. The Bayesian analogue is the second order random walk smoothness priors of the form:

$$\beta_{jk,rd} = 2\beta_{jk,r,d-1} - \beta_{jk,r,d-2} + \varepsilon_{jk,rd}, d = 3,4,...,D \quad (7)$$

with iid Gaussian errors $\left(\varepsilon_{jk,rd} \sim N\left(0, \tau^2_{jk,\varepsilon}\right)\right)$ where $\tau^2_{jk,\varepsilon} = 1/\sigma^2$. The linear trend coefficients' initial values of the random walk were assigned diffuse priors, $P(\beta_{jk,r1}) \propto const$ and $P(\beta_{jk,r2}) \propto const$.

The *spatial effects* were modelled separately to distinguish between the different effects on the outcome, that is, $f_{jk,spat}(t)(s_i) = f_{jk,str}(t)(s_i) + f_{jk,unstr}(t)(s_i)$. For the spatial correlated (structured) effects $\left(f_{jk,str}(t)(s)\right)$ we assumed a GMRF [16] prior. In this case, we defined areas as neighbors if they share a common boundary and assume that the effect of an area $s \in \{1,2,3,...,S\}$ is conditionally Gaussian. The spatial smoothness prior for the spatial function evaluation $f_{jk,str}(s) = \beta^{str}_s$ is given by:

$$f_{jk,str}(s) = \beta^{str}_s = \frac{1}{N_s}\sum_{s' \in \partial_s} \beta_{s'} + u_s, u_s \sim N\left(0, \frac{\boldsymbol{\tau}^2_{jk,str}}{N_s}\right) \quad (8)$$

where $s' \in \partial_s$ denotes that province s' is a neighbor of province s. The conditional mean of β_s is an unweighted average of function evaluations of neighboring provinces. The number of parameter D equals the number of distinct areas S and the $n \times S$ design matrix Z_{str} is a 0-1 incidence matrix. Its values on the ith row and sth column is a one if an observation is located in the province s and zero otherwise. The $S \times S$ penalty matrix W_{str} has the form of the adjacency matrix with $rank(W_{str}) = S - 1$. The dimension of the penalty matrix in GMRF equals to the number of different spatial regions (provinces in our case) S; hence, the computational burden is less compared to the stationary GRF priors approach. The *unstructured spatial effects* $f_{unstr}(s)$ were assumed to be iid Gaussian priors, $f_{unstr}(s) \sim N(0, \tau^2_{unstr})$. In real situations, usually it is not known how much spatial variation is explained by both the structured and the unstructured effects; therefore, the interpretation of the spatial effects is based on the sum of these two effects.

The variance parameter vector $\boldsymbol{\tau}^2_{jk,q} = \left(\tau^2_{jk,1}, \tau^2_{jk,2}, ..., \tau^2_{jk,y}\right)'$ for $q = 1,2,...,y$ contains variance parameters for the error term $\tau^2_{jk,\varepsilon}$, frailty term $\boldsymbol{\tau}^2_{jk,b}$, structured spatial terms $\tau^2_{jk,str}$, the unstructured spatial terms $\tau^2_{jk,unstr}$ and the generic random effects (regression) coefficients $\tau^2_{jk,r}$. Routinely, each of these variance hyperparameters is assigned a non-informative inverse Gamma priors with known parameter values a=b= 0.001, that is, $\left(\tau^2_{jk,q} \sim IG\left(a_q, b_q\right)\right)$

$$P\left(\boldsymbol{\tau}^2_{jk,q}\right) \propto \frac{1}{\left(\boldsymbol{\tau}^2_{jk,q}\right)^{a_q+1}} \exp\left(\frac{b_q}{\boldsymbol{\tau}^2_{jk,q}}\right), \text{for } a_q, b_q > 0 \quad (9)$$

Additional information is given in the Appendix 7.

2.4. Posterior Distribution

The fully Bayesian inference is based on the entire posterior distribution, and more detail is shown in Appendix 8:

$$P\left(\boldsymbol{\beta},\boldsymbol{\gamma},\boldsymbol{\tau}^2 / data\right) \propto L\left(data / \boldsymbol{\beta},\boldsymbol{\gamma},\boldsymbol{\tau}^2\right) P\left(\boldsymbol{\beta},\boldsymbol{\gamma},\boldsymbol{\tau}^2\right) \tag{10}$$

The likelihood as defined in Section 2.2 and the joint prior made up of the individual prior distributions of the specified parameters yield the posterior distribution. Due to conditional independence assumptions, the joint prior factorizes into:

$$P\left(\boldsymbol{\beta},\boldsymbol{\gamma},\boldsymbol{\tau}^2\right) = \left\{\prod_{r=0}^{m} P\left(\beta_{jk,r} / \tau^2_{jk,q}\right) P\left(\tau^2_{jk,q}\right)\right\} P\left(\boldsymbol{\gamma}\right) \propto$$
$$\left\{\prod_{q,r=0}^{m} \frac{1}{\left(\tau^2_{jk,q}\right)^{a_q+1}} \exp\left(\left(\frac{b_q}{\tau^2_{jk,q}}\right) - \frac{\beta'_{jk,r} W_{jk,r} \beta_{jk,r}}{2\tau^2_{jk,q}}\right)\right\} \tag{11}$$

The component $P\left(\boldsymbol{\gamma}\right)$ can be omitted since it represents fixed effects prior. The posterior distribution $P\left(\boldsymbol{\beta},\boldsymbol{\gamma},\boldsymbol{\tau}^2 / data\right)$ is then an approximation of the product of Equation (5) and (11).

2.5. Markov Chain Monte Carlo Inference

Since this posterior distribution is not in a closed form, we used the MCMC simulation method based on updating full conditionals of single parameters or blocks of parameters (for the same transition rate), given the rest of parameters and data. To update the parameter vector $\boldsymbol{\beta}_{jk,r}$ which corresponds to the time-independent functions, spatial effects, fixed effects and random effects; we used the Metropolis-Hastings (MH) algorithm based on iteratively weighted least squares (IWLS) proposals for generalized linear mixed effects models (GLMM) [17] and adapted to generalized structure additive models (GSAM) [18]. Suppose we want to update $\boldsymbol{\beta}_{jk,r}$ with current value $\boldsymbol{\beta}^c_{jk,r}$ of the chain, the new value $\boldsymbol{\beta}^p_{jk,r}$ is proposed by drawing a random vector from the high-dimensional multivariate Gaussian proposal distribution $q\left(\boldsymbol{\beta}^c_{jk,r}, \boldsymbol{\beta}^p_{jk,r}\right)$ which is attained from the quadratic approximation to the posterior by a second-order Taylor expansion with respect to $\boldsymbol{\beta}^c_{jk,r}$ explicitly illustrated in Appendix 9. Other parameters corresponding to the time-varying log-baseline effects were estimated using a computationally faster MH-algorithm based on conditional prior proposals. Unlike the ILWS algorithm which requires derivatives, MH-algorithm requires the evaluation of the log-likelihood since the derivatives are computationally intensive for these parameters due to the additional integrals involved. As the full conditionals of the variance parameters are inverse Gamma distributions, updating the hyper-parameters was done using Gibbs sampling.

2.6. Model Diagnostics and Sensitivity Analysis

The convergence of the Markov chains to their stationary distributions was assessed by inspecting the sampling paths and autocorrelation functions of the sampled parameters. Trace plots and visual autocorrelation plots were used to evaluate the performance of the model. In running the MCMC algorithm, 10,000 iterations were made with a burn-in of 2,000 and a thinning parameter of 20. We also performed a sensitivity analysis to ensure that the choice of the priors did not have an influence on the obtained results. In the initial run, default Gamma priors with hyper-parameters $\left(\alpha = \beta = 0.001\right)$ were used then two more trials using values of $\alpha = \beta = 0.0001$ and $\alpha = 1 \text{ with } \beta = 0.001$. The results reported are those of the model with default prior values.

3. APPLICATION OF THE MODEL

3.1. The Zimbabwe National ART Programme Data

The national ART programme was introduced in Zimbabwe in 2004 to provide treatment for PLWHIV and support the fight against HIV [19]. Patients' data are routinely collected at ART initiation, and subsequent follow-up visits, through the electronic patient management system (ePMS) [20]. The ePMS was introduced to improve and increase efficiency in patient monitoring compare to the paper-based system and allows analysis at the national level of suitably anonymized patient data.

At baseline, demographic and clinical information is captured including gender, age, and WHO clinical stage, while viral load and CD4 measurements are captured at baseline as well as in subsequent visits. WHO recommends the use of laboratory monitoring to manage HIV patients on ART, using viral load measurements at baseline (6 months after ART initiation) and then every six months to guide patient management. Practically, this patient-level information is taken intermittently over time; hence, missing data is common due to patients' travels, patients' social circumstances, patients' treatment non-adherence or errors during data capturing. Missing data in program data may also be due to program guidelines and policies, the data used in this study covers the period when differential monitoring was done [21]. These aspects lead to missing and irregular compilation of

longitudinal data points which are likely to be missing not at random (MNAR). In this study, we considered primarily those individuals who had at least two subsequent viral load measurements.

3.2. Study Design and Ethics

This study was a secondary data analysis of a retrospective cohort of anonymous HIV positive patients initiated on ART between 2004 and 2017, and whom their routine data was captured through the ePMS system linked with the Zimbabwean Ministry of Health and Child Care (ZMOHCC). Permission to use the data was obtained from ZMOHCC, and ethical clearance was granted by the University of Witwatersrand's Human Research Ethics Committee (Medical) (Clearance Certificate No. M170673).

4. RESULTS

4.1. Descriptive Analysis of the Baseline Characteristics

Of the 18,150 participants with two or more viral load measurements following ART initiation: 64.3% (n=11,671) participants had detectable viral load (>50copies/mL) while 35.7% (n=6,479) had undetectable viral load (<50copies/mL). There was a significant difference between these baseline proportions of patients with undetectable viral load and those with detectable viral load, p-value<0.001. The mean (standard deviation) age and weight was 39.1(10.2) years and 62.4(13.5) Kgs at ART initiation, respectively. Majority of the patients were females (67.1%), enrolled at the primary health care (PHC) facilities (68.2%) within rural areas (52.4%). Majority of the patients were on first-line regimen (95.0%) and 53.3% in WHO clinical stage III/IV. Most of the patients did not move out of their initially occupied state, particularly the viral rebound state (68.74%). A total of 496 patients (2.73%) had died at the end of the study (Table **1**).

4.1. Fully Bayesian Time-Varying Transition Intensities Pattern Results

We fitted an unadjusted (no covariate) and covariate adjusted models to obtain the time-varying log-baseline hazard plots. The unadjusted model gave

Table 1: Participants' Baseline Characteristics (Sociodemographic and Clinical) and the Observed Transitions during the Follow-Up Period in the Zimbabwe National ART Programme, 2004-2017

Variable	Category	Frequency	Percentage
Health facility type	Primary Health Care	12 385	68.24
	District /Mission hospital	4 527	24.94
	Provincial/Referral hospital	1 238	6.82
Degree or urbanization of health facilities	Rural	9 700	53.44
	Urban	8 450	46.56
Sex	Female	12 169	67.05
	Male	5 981	32.95
Regimen type	First line	17 234	94.95
	D4T(30)+ 3TC+NVP	9	0.05
	AZT+3TC+NVP	353	1.94
	AZT+3TC+EFT	38	0.21
	TDF+3TC+NVP	280	1.54
	AZT+3TC+EFV	16 554	91.21
	Second line	916	5.05
WHO clinical states	I/II	7 700	42.42
	III/IV	9 679	53.33
	Missing	771	4.25
Baseline viral load states	Suppressed state (State 1)	6 401	35.27
	Unsuppressed state (State 2)	11 749	64.73
Transitions between states	$1 \rightarrow 1$	21 645	24.39
	$1 \rightarrow 2$	2 803	3.16
	$1 \rightarrow 3$	200	0.23
	$2 \rightarrow 1$	2 804	3.16
	$2 \rightarrow 2$	61 015	68.74
	$2 \rightarrow 3$	296	0.33

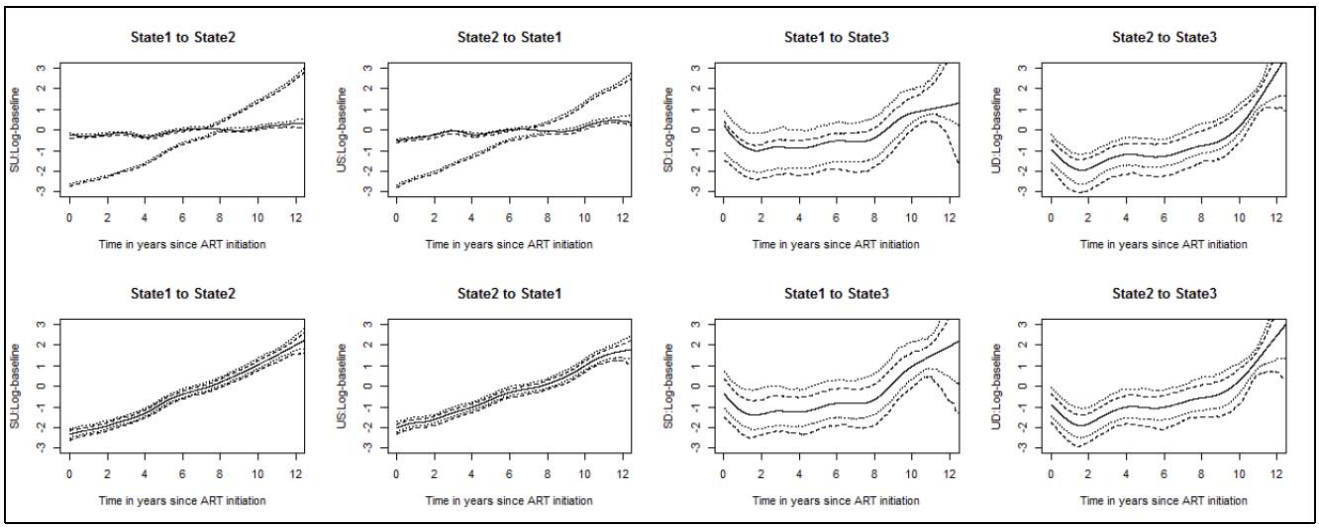

Figure 2: Estimated time-varying log-baseline transitions (middle line) and their 95% and 80% credible intervals from the fully Bayesian inference estimation of univariate analysis/no covariates (top panel) and multiple covariate model with non-linear, fixed and spatial covariates (bottom panel).

wide credible intervals (CI) for both the viral rebound (undetectable (state 1) to detectable (state 2)) and viral suppression (detectable (state 2) to undetectable (state 1)) transitions as shown in Figure **2** (top panel). Adjusting for the other covariates narrowed the time-varying log-baseline CI. Therefore, we reported results based on the adjusted model Figure **2** (bottom panel). We observed an increase in the log-baseline hazard rates with time since ART initiation for both the viral suppression (state 2 to state 1) and viral rebound (state 1 to state 2) transitions. The two time-varying log-baseline mortality transition rates steadily increased with time.

Comparing the viral suppression (state 2 to state 1) and viral rebound (state 1 to state 2) transitions on one plane, we observed that the log-baseline effects of attaining viral suppression (state 2 to state 1) were higher from ART initiation till the 7.2 year mark before going down thereafter (Figure **3a**). The log-baseline hazard rates of mortality from either state showed a fluctuating pattern over time (Figure **3b**). Among virally suppressed (state 1) patients, the risk of attaining viral suppression was higher in the early years of ART initiation compared to the risk of attaining viral rebound; however, after the 10 year mark, there was no difference between the two transitions (Figure **3c**). Contrary, among the patients who attained viral rebound (state 2), the risk of regaining immune recovery was higher than that of death in overall (Figure **3d**).

Table **2** presents the results of the effects of the fixed covariates on each of the transitions. Although the effects of WHO clinical stage were not significant for the viral suppression (state 2 to state 1) transition and on the risk of death from any state; patients in WHO clinical stage III/IV had a higher risk of a viral rebound compared to those in WHO I/II (posterior hazard ratio (PHR) =1.26; 95%CI: 1.03-1.48). Compared to females, male patients were 64% times less likely to attain a viral rebound (PHR=0.36; 95%CI: 0.29-0.45); 1.57 times (95%CI: 1.28-1.90) more likely to become virally suppressed and 1.68 times (95%CI: 1.32-2.05) more likely to die if they have a viral rebound. However, there was no significant difference in gender on the risk of death if an individual was virally suppressed.

The effects of age on the risk of the four transitions are presented in Figure **4**. The age effects on the risk of mortality and viral rebound for an individual with suppressed viral load was high if a patient was either an adolescents/young adult (below 30years) or older (above 60years) as shown by the bath-tub "∪" shaped splines; however, the effects for older patients were not significant due to fewer numbers of participants in this category. Contrarily, the age effects on the risk of viral suppression followed a doom "∩" shape. This means individuals aged 30-60 years with viral load rebound had a higher risk of experiencing the reverse transition and subsequently attaining viral suppression. Also, the age effects on the risk of mortality for an individual with viral rebound increased with an increase in age until 30 years before remaining constant thereafter.

The smooth geographical effects are shown in Figure **5** with their corresponding 95%CI for each transition based on Zimbabwe provinces as the spatial

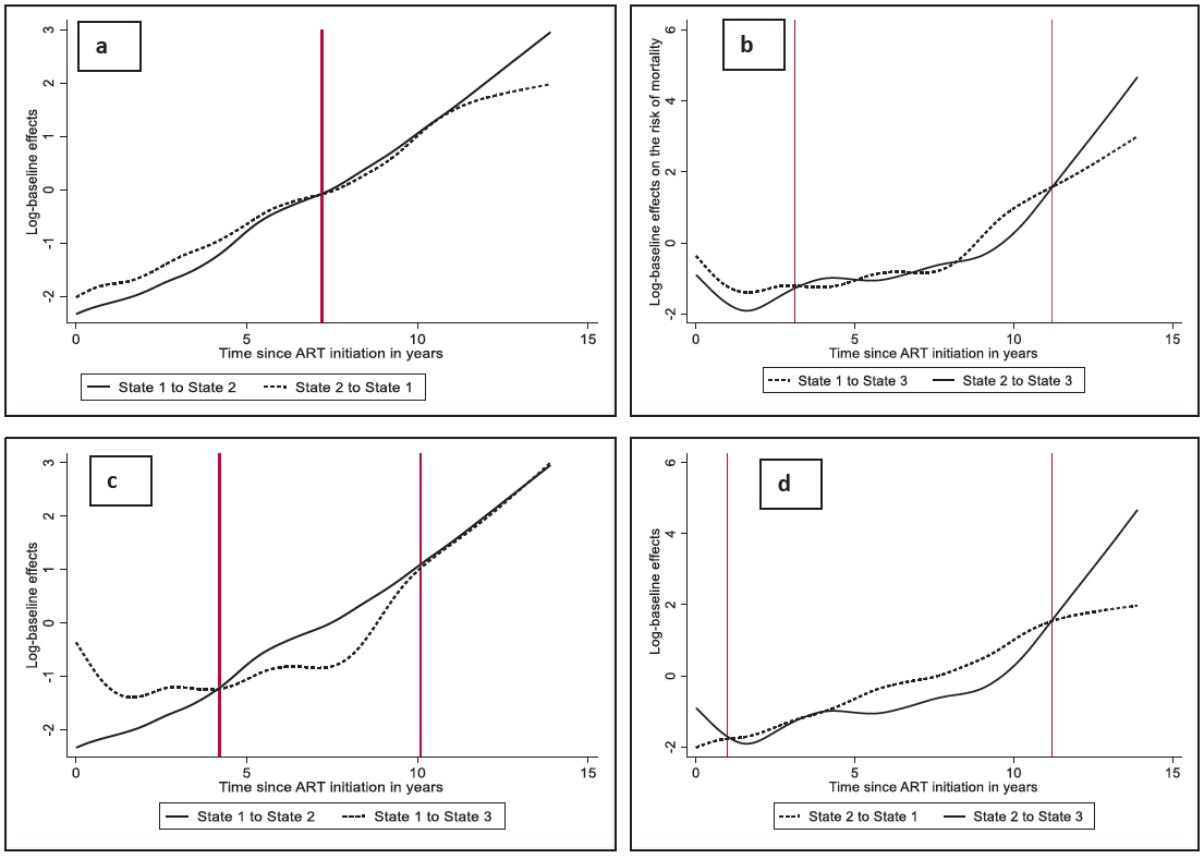

Figure 3: Comparison of the estimated time-varying log-baseline transitions from the fully adjusted Bayesian multistate model.

Table 2: Fixed Effect Covariates Results for the Estimated Transition Intensities Coefficients and Ratios in the Zimbabwe National ART Programme Based on Viral Load Measurements, 2004 to 2017

Covariates Transitions		WHO III/IV (Reference: WHO I/II) Mean(95% Credible Intervals)	Sex (Reference: Female) Mean(95% Credible Intervals)
Viral rebound (state 1 to 2)	Coefficients	0.23 (0.03 to 0.39)*	-1.02 (-1.24 to -0.79)*
	Exponents	1.26 (1.03 to 1.48)*	0.36 (0.29 to 0.45)*
Viral suppression (state 2 to 1)	Coefficients	-0.12 (-0.29 to 0.04)	0.45 (0.25 to 0.64)*
	Exponents	0.89 (0.75-1.04)	1.57 (1.28-1.90)*
Viral suppression mortality (state 1 to 3)	Coefficients	0.19 (-0.11 to 0.51)	-0.17 (-0.49 to 0.11)
	Exponents	1.21 (0.90-1.67)	0.84 (0.61-1.12)
Viral rebound mortality (state 2 to 3)	Coefficients	-0.43 (-0.53 to 0.17)	0.52 (0.28 to 0.76)*
	Exponents	0.65 (0.59-1.19)	1.68 (1.32-2.05)*

*Significant at 5%.

unit. The yellow colour represents regions with non-significant spatial effects for all the transitions. For the risk of viral rebound and the risk of mortalities from either state, the red colour indicates an increased spatial effect while green colour indicates a decreased spatial effect. The region which borders with Botswana and Zambia (Matabeleland North province) had a significant highest likelihood of viral rebound (state 1 to state 2) transition compared to other regions. For the risk of viral suppression, the red colour indicates decreased spatial effects while green colour indicates increased spatial effects. The southern region which borders with Botswana, the middle region in the central parts of the country and northern regions bordering Zambia and Mozambique had a low likelihood of the viral suppression (state 2 to state 1) transition. This

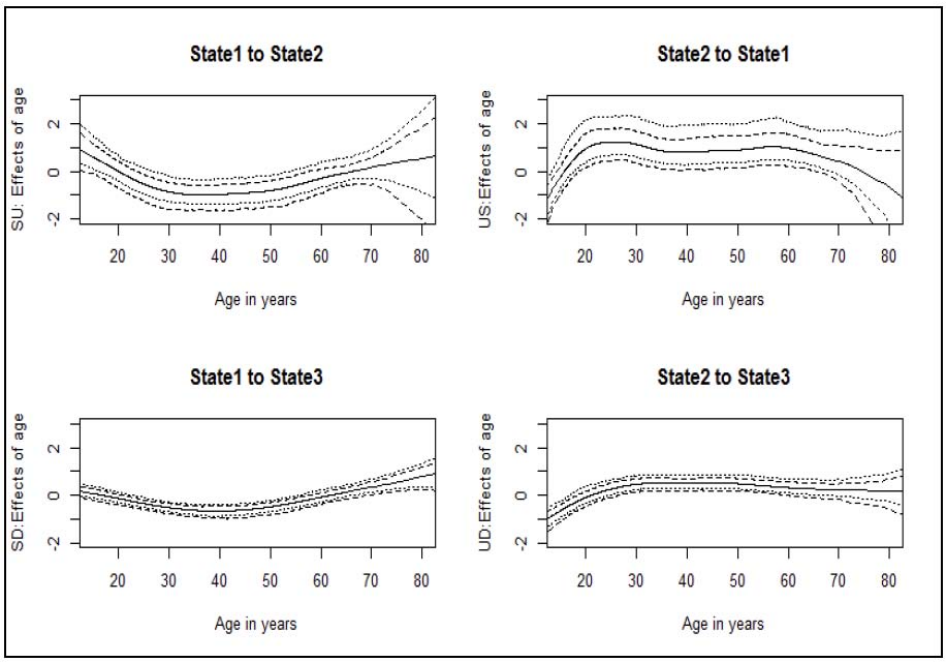

Figure 4: Estimated nonparametric effects of the continuous covariate (age) (middle line) and their 95% and 80% credible intervals from the fully Bayesian inference for the four transitions.

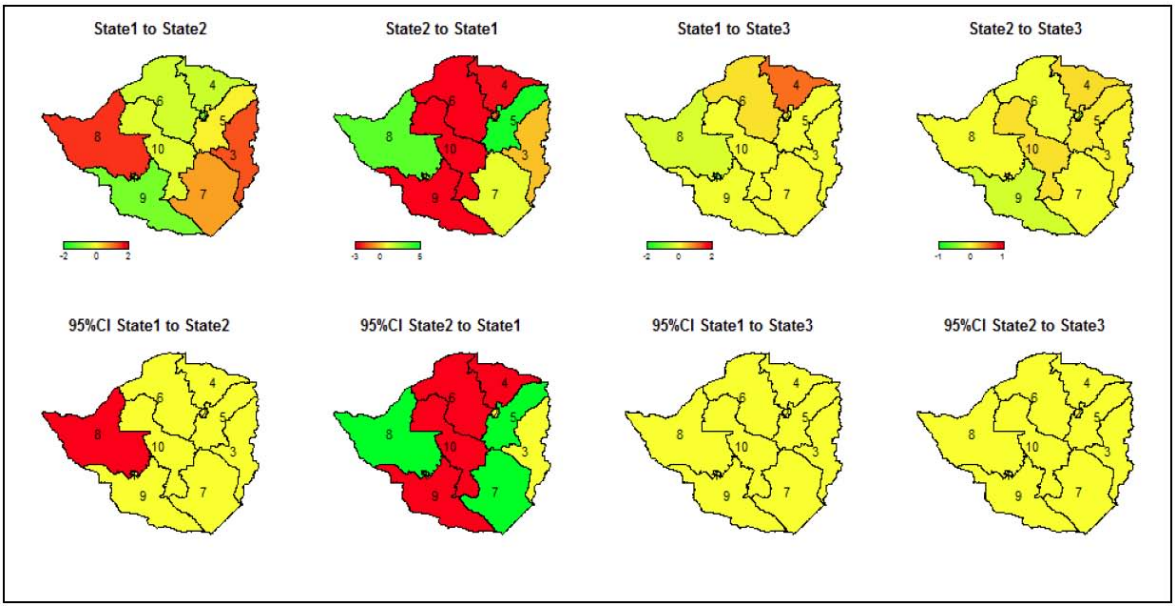

Figure 5: Smooth spatial effects posterior means of provinces in Zimbabwe (top panel) and their corresponding 95% credible intervals (bottom panel) from the fully Bayesian inference [1-Bulawayo, 2-Harare, 3-Manicaland, 4-Mashonaland Central, 5-Mashonaland East, 6-Mashonaland West, 7-Masvingo, 8-Matabeleland North, 9-Matabeleland South, 10-Midland].

means that patients in these regions were less likely to attain undetectable viral suppression compared to other regions.

5. DISCUSSION

The aim of this study was to determine the spatial heterogeneity of viral suppression and viral rebound trajectories from a subset of the Zimbabwe national ART programme data using a Bayesian geoadditive multistate model. To our knowledge, this is the first application of spatial effects within the multistate models' framework since none of the models in the original design has included the spatial random effects. Use of Bayesian multistate models in HIV studies is also scarce in the literature compared to the maximum likelihood multistate models; however, these Bayesian models are equally robust despite being

computationally intensive. Bayesian models give more comprehensive information through the use of priors which results in much more precise estimates as compared to the frequentist models [7]. Moreover, the spatial modelling has not been fully utilized in HIV monitoring to guide policy, particularly in resource constrained areas. We observed variations on viral suppression and viral bound transition patterns by geographical region, age, gender and WHO status in this cohort.

5.1. Epidemiological Discussion

The study findings showed that the log-baseline hazard rates for the viral load suppression to undetectable levels (state 2 to state 1) transition were as expected. The longer the patient was on ART, the more likely that patient was to attain viral suppression to undetectable levels. This is a good indication of how ART helps one to regress to a better state with time by improving viral suppression. This finding affirms the primary objective of ART which is to sustain viral suppression, decrease HIV transmission and improve survival outcomes of the individuals through immune function reconstitution [22]. Moreover, attaining a viral suppression is crucial for PLWHIV so that their life expectancy can be comparable to HIV-uninfected population [22]. The study results also assert that patients who are initiated on ART with advanced illness tend to adhere to their medication anticipating to recover and prolong their lives together with their families [23]. Surprisingly, male patients were more likely to attain viral suppression compared to female patients; however, male patients with high viral load measurements were more likely to die than recover. The higher risk of mortality among males can be explained by their association with poor immunological response to treatment resulting in death [24]. Male patients also have poor health-seeking behaviour compared to females which may result in late HIV diagnosis and delayed ART initiation [25]. To achieve and sustain viral suppression, interventions which minimize mortality, target high-risk behaviour changes and increase the gravity of ART adherence are crucial for males. For instance, rapid roll-out and promotion of self-testing campaigns [26] may be considered for people who do not usually seek voluntary HIV testing in health facilities to promote community-based testing among male subpopulation [27, 28]. The 30-60 years aged patients showed a higher effect of attaining viral suppression in this study, while adolescents and young adult subpopulations showed lower effects. This finding aligns with previous studies indicating that adolescents and young adult subpopulations experience suboptimal clinical outcomes and face different challenges which may result in treatment non-adherence [22]. The adolescence group is also known to be vulnerable as they are in the dynamic life transition of becoming independent [29]. Young adults group may not fully understand the gravity of ART adherence; hence, health care and social service providers should compassionately offer continual counselling support to improve young adults' retention.

The log-baseline hazard rates for the viral rebound transition also increased with increase in time. In the presents of potent and effective ART treatment, it would be logical to expect a decrease in the viral rebound (state 1 to state 2) transition rates over time; however, this was not the case in this study. The results assert that sustaining viral suppression is still a challenge in HIV treatment. This finding can be explained by the fact that once individuals attain viral suppression, they may think that they are fully healthy again and no longer see the importance of continual treatment intake. This results in treatment interruptions which can trigger treatment defaulting, non-adherence, failure or resistance [30, 31]. Other studies have shown that majority of patients who attain a viral rebound with low CD4 cell counts are more likely to experience poor ART outcomes like HIV disease progression, loss to follow-up and mortality resulting in poor patient retention in HIV care [3, 22].

Interestingly, this study observed that adolescence and young adults aged below 30 years were found to have a higher risk of viral rebound. This finding supports previous studies that have shown that adolescents and young adults are less likely to achieve and sustain viral suppression [32]; hence, their risk of mortality is higher than older patients [3]. This finding can be explained by the fact that the below 30 years age group faces different life encounters which may lead to treatment non-adherence putting them at risk of unsustained viral load suppression and consequently viral rebound [22]. We also observed that older patients aged 60 years and above had a high risk of attaining viral rebound in this cohort. This can be explained by the fact that this group is associated with non-communicable comorbidities like hypertension diabetes and cancers in addition to communicable illnesses like tuberculosis associated with HIV infection [33]. These comorbidities result in multiple drug toxicity which may trigger non-adherence and subsequently viral rebound. Therefore, pharmacological services should aim to continue providing potent and effective ART regimens

with minimum side-effects and less prone to resistance to achieve treatment adherence and viral suppression. Not only can viral rebound results in death outcomes but also in an upsurge in vulnerability to opportunistic infections since the immune system becomes weaker; and this is supported by the observed high risk of viral rebound among patients with advanced WHO clinical stages in this study.

The smooth spatial effects show that patients from the Matabeleland North province had a higher risk of viral rebound. This finding could be supported by the fact that this region has a lot of movement of residents to Botswana and Zambia seeking jobs or informal trading which may attribute to poor retention and subsequently poor treatment adherence. Moreover, due to tourism activities which attract diverse people and the existence of the long truck route connecting into neighbouring countries, this region has a high risk of multiple sex partners [34] and is prone to sex for money activities [35] which may contribute to acquiring new HIV strains. This becomes a threat to viral suppression and promotes viral rebound through ART resistance or failure resulting in the need of a different HIV regimen. Besides, the viral rebound spatial patterns depicted in this region could be due to non-adherence to treatment yielding from poor provider-patient relationships; therefore, professional training of service providers on the proper code of conduct towards HIV patients is critical. Another reason could be the short treatment dispensary period of 3 months, especially for informal traders to neighbouring countries; hence, revising these guidelines to 6 months can be an option. Also, rural residents in this region may face transport challenges due to the poor road networks and terrain. Interventions like ART adherence clubs functional mobile clinics, community-based dispensing points or other optional ART distribution strategies for these communities may be of benefit [36,37]. The smooth spatial effects for viral suppression show that patients from the intra-regions stretching from the Botswana border to Zambia/Mozambique border were less likely to attain viral suppression. This finding could be explained by late presentation leading to delayed ART initiation [38,39]; hence, immune recovery becomes slow in most instances. Interventions which were found to be effective include strengthening and intensifying index testing, lay testing and community mobilization for testing-HIV musical galas campaigns in addition to self-testing campaigns [27, 28].

5.2. Statistical Discussion

Our modelling approach incorporated the spatial random effects in the flexible predictor of the multistate model. This controlled for unobserved heterogeneity in addition to individual random effects which frequentist models cannot handle [40]. Such modelling approaches in epidemiological studies are of importance to get unbiased estimates as they reflect reality. This convolution modelling approach of the spatial component was preferred since it fully accounts for the spatial correlation and address essential public health aspects that are beyond the scope of a simple pictorial analysis [41]. Moreover, time-varying transition intensities were considered to account for the dynamic natural events.

Our findings should be interpreted cautiously; participants used in this study were conveniently sampled from the Zimbabwe national ART program ePMS database on the basis of having two consecutive viral load measurements leading to participant selection bias. This small sample might not be a true representation of all ART patients in Zimbabwe over this period in time and may negatively impact on the generalizability and inference of the observed results. This means the data should be viewed as a non-random representation from all those who are on ART in Zimbabwe. Relatively few death outcomes were observed in this study which could be due to under-reporting of the deaths in the ePMS database; hence, it is likely that the mortality transitions were underestimated in this study. Moreover, the model used assumed right censoring of observations since it cannot support interval censoring. However, going forward the statistical analysis approach used provides useful information to epidemiologist, patients and policymakers on the spatial variations of viral load transitions for HIV/AIDS disease progression and death.

This study acknowledges how ART policies have been changing over the years. ART regimen prescription has changed from multiple-tablets daily regimen to single-tablet once daily regimens. The impact of the single-tablet once daily regimens prescription has resulted in improved adherence, improved patient satisfaction and improved virological response [42,43]; however, this study could not adjust for these time-varying covariates since they were not available in the analysed data. Also, there have been changes in ART monitoring policy moving from WHO clinical monitoring to CD4 cell counts monitoring and

now the use of viral load monitoring. The overall policy impact of using viral load monitoring has resulted in a faster switch of ART regimen when treatment failure is indicated from first-line to second-line therapy [44]. This subsequently leads to patients attaining viral suppression and reduced HIV transmission; however, most developing countries still have centralized laboratories which can be logistically challenging to meet WHO recommendations to measure viral load at baseline and after every 6 months [44, 45]. Over the years, most resource-limited settings including Zimbabwe have been doing differential monitoring targeting those patients with clinical signs which require viral load assessment as recommended by the clinician. This means, after achieving viral suppression, most of these patients did not have another viral load measurement taken until they had clinical signs which justify a viral load measurement to be taken. This differential monitoring approach may give biased inferences through participants' selection bias since we are likely to have considered predominantly those patients with conditional viral load measurements based on the physician discretion. However, since 2016, there have been significant strides towards viral loads measurements monitoring are per WHO recommendations for HIV monitoring in Zimbabwe [46].

We also did not consider ART adherence in this study which is an important predictor of viral suppression and viral rebound since it was not measured in the data; therefore, future research should consider these influential variables. Additionally, the difference between the spatial regions in viral suppression or viral rebound patterns may be due to the small sample sizes of participants in these regions which might not completely represent the regional picture had the estimates been weighted or sample size increased. However, our results for the spatial viral rebound transitions align with the national surveys in that, the region we found to have the highest likelihood of viral rebound was ranked the second-highest HIV prevalence region in ZIMPHIA 2015/16 national survey [46]. This affirms that regions with high viral rebound are susceptible to high risk of viral transmission leading to high HIV infections in the general population. Moreover, the differences in health facilities which offer ART services in Zimbabwe could have influenced the observed results in that, regions with fewer dispersed health facilities are associated with poor HIV disease progression outcomes since access to treatment is not as easy as those regions with multiple health facilities. Besides, health facilities in urban or cities usually perform better in terms of ART patients support and service provision compared to rural health facilities. However, despite these limitations, important information regarding viral suppression and viral rebound transitions and the associated spatial heterogeneity patterns were determined; and the subpopulation groups of people with a high risk of suboptimal viral rebound and mortality were also identified using the Bayesian geoadditive multistate model.

6. CONCLUSION

This study demonstrated the first inclusion of spatial random effects in Bayesian multistate models' framework implemented in the C++ BayesX free software and we observed that the viral suppression transitions were not static. The inclusion of spatial effects in multistate models is of profound relevance in resource-limited settings in the evolving modelling techniques. Structured maps are useful for policymakers to visually identify high-risk regions and interventions on those areas unveiling eminent outcome risk [47]. Further studies need to consider the effects of CD4 cell counts on the viral load suppression and rebound transitions to get improved outcomes from a Bayesian perspective [4]; adjust for the effects of time-varying covariates like regimen change on the viral suppression and viral rebound transition; consider regional donor funds or HIV interventions to get much more informative findings. Also, the viral suppression and viral rebound spatial correlation can be extended to district levels spatial units or different subpopulation groups to precisely guide targeted intervention to specific subpopulation groups.

Suboptimal adherence and poor retention in care increase the risk of viral rebound, particularly among adolescents and young adult subpopulation. Holistic intervention approaches which may be considered include self-monitoring, peer support, patient follow-ups, treatment refill mobile phone reminders, and patient and caregiver educational support. Health literacy and belief are significant barriers to ART adherence; hence, interventions which include education sessions on ART addressing the negative effects of beliefs in divine healing, the inclination for traditional medicine and misconceptions over ART benefits and safety are crucial to achieve and sustain viral suppression. Moreover, models which expedite treatment uptake for the newly diagnosed patients coupled with tailored approached for adolescents, young adults and male subpopulations should be

developed to promote early diagnostics and ART uptake, reduce barriers to care and subsequently to achieve optimal health of these subpopulations. Most promising interventions which improve ART adherence and patient retention in care through minimizing "leakages" in the HIV continuum of care cascade are essential for all patients in care and should be the focus of HIV treatment and prevention in the pursuit of the UNAIDS 90-90-90 fast track targets.

ACKNOWLEDGEMENTS

Our acknowledgements go to the Ministry of Health and Child Care, AIDS/TB Units department for the support and compilation of the data used in this study. We also thank the Division of Epidemiology and Biostatistics at the School of Public Health for their assistance in the getting ethical approval of this study. Thanks to Professor Thomas Kneib for quick responses during the development of the manuscript and sharing helpful material for the analysis.

This work was supported by the Developing Excellence in Leadership, Training and Science (DELTAS) Africa Initiative Sub-Saharan Africa Consortium for Advanced Biostatistics (SSACAB) [Grant No. 107754/Z/15/Z]. The DELTAS Africa Initiative is an independent funding scheme of the African Academy of Sciences (AAS) Alliance for Accelerating Excellence in Science in Africa (AESA) and is supported by the New Partnership for Africa's Development Planning and Coordinating Agency (NEPAD Agency) with funding from the Wellcome Trust [Grant No. 107754/Z/15/Z] and the United Kingdom government. The views expressed in this publication are those of the authors and not necessarily those of the AAS, NEPAD Agency, Wellcome Trust, the UK government or Ministry of Health and Child Care, Zimbabwe.

AUTHOR'S CONTRIBUTION

ZMZ conceived the idea and performed all the analyses. EM guided and oversaw the analysis. ZMZ, EM, JT and TFC contributed to the interpretation of the results. ZMZ drafted the manuscript. All authors reviewed the manuscript critically for and approved the final version submitted for publication.

SUPPLEMENT MATERIAL

The supplemental materials can be downloaded from the journal website along with the article.

CONFLICT OF INTEREST

The authors declare that they have no competing interests for this work.

REFERENCES

[1] Meira-Machado L, Uña-Álvarez JDe, Cadarso-Suárez C, Andersen PK. Multi-State Models For The Analysis Of Time-To-Event Data. Statistical methods in Medical Research 2009; 18(2): 195-222. https://doi.org/10.1177/0962280208092301

[2] Jackson CH. Multi-State Models For Panel Data: The Msm Package For R. Journal of Statistical Software 2011; 38(8): 1-28. https://doi.org/10.18637/jss.v038.i08

[3] Matsena Z, Zvifadzo C, Tobias F, Todd J, Musenge E. HIV Disease Progression Among Antiretroviral Therapy Patients In Zimbabwe : A Multistate Markov Model. Frontiers in Public Health 2019; 7: 1-15. https://doi.org/10.3389/fpubh.2019.00326

[4] Shoko C, Chikobvu D. A Superiority Of Viral Load Over CD4 Cell Count When Predicting Mortality In HIV Patients On Therapy. BMC Infectious Diseases 2019; 19(1): 1-10. https://doi.org/10.1186/s12879-019-3781-1

[5] Kneib T, Hennerfeind A. Bayesian Semiparametric Multi-State Models. Statistical Modelling 2008; 8(2): 169-198. https://doi.org/10.1177/1471082X0800800203

[6] Eilers PHC, Marx BD. Flexible Smoothing With B-Splines And Penalties. Statistical Science 1996; 11(2): 89-121. https://doi.org/10.1214/ss/1038425655

[7] Odhiambo C, Kareko MJ. An Evaluation Of Frequentist And Bayesian Approach To Geo-Spatial Analysis Of HIV Viral Load Suppression Data. International Journal of Statistics and Applications 2019; 9(6): 171-179.

[8] UNAIDS. 90-90-90 An ambitious treatment target to help end AIDS epidemic. United Nations 2014. URL http://www.unaids.org/sites/default/files/media_asset/90-90-90_en.pdf[Accessed 25 January 2019]

[9] Ministry of Health and Child Care, National AIDS Council. Global Aids Response Progress Report 2018 Gam Zimbabwe Country Report 2017. URL http://www.unaids.org/sites/default/files/country/documents/ZWE_2018_countryreport.pdf [Accessed on 27 September 2018]

[10] UNAIDS. Undetectable = Untransmittable Public Health and HIV viral load suppression 2018. URL http://www.unaids.org/sites/default/files/media_asset/undetectable-untransmittable_en.pdf [Accessed 5 February 2019]

[11] StataCorp. Stata Statistical Software: Release 15. College Station, Texas, USA 2017.

[12] Belits C, Brezger A, Klein N, Kneib T, Lang S, Umlauf N. BayesX - Software For Bayesian Inference In Structured Additive Regression Models 2015.

[13] RStudio Team. RStudio: Integrated Development For R. RStudio, Inc. Boston, USA 2015.

[14] Friedman M. Piecewise Exponential Models For Survival Data With Covariates. The Annals of Statistics 1982; 10(1): 101-113. https://doi.org/10.1214/aos/1176345693

[15] Fahrmeir L, Kneib T, Lang S. Penalized Structure Additive Regression For Space-Time Data: A Bayesian Perspective. Statistica Sinica 2004; 14: 715-745.

[16] Besag J, York J, Mollie A. Bayesian Image Restoration, With Two Applications In Spatial Statistics. Annals of the Institute of Statistical Mathematics 1991; 43(1): 1-59. https://doi.org/10.1007/BF00116466

[17] Gamerman D. Sampling From The Posterior Distribution In Generalized Linear Mixed Models. Statistics and Computing 1997; 7: 57-68. https://doi.org/10.1023/A:1018509429360

[18] Brezger A, Lang S, Brezger Lang. Generalized Structured Additive Regression Based On Bayesian P-Splines Projektpartner Generalized Structured Additive Regression Based On Bayesian. Computational Statistics & Data Analysis 2006; 50(4): 967-991. https://doi.org/10.1016/j.csda.2004.10.011

[19] Apollo T, Takarinda K, Mugurungi O, Chakanyuka C, Simbini, T, Harries AD. A Report On The Zimbabwe Antiretroviral Therapy (ART) Programme Progress Towards Achieving MGD6 Target 6B: Achievement And Challenges. The Central African Journal of Medicine 2010; 56(1-4): 12-14.

[20] Ministry of Health and Child Care. Zimbabwe Electronic Patient Management System Strategic Plan Document 2012.

[21] Phillips A, Vojnov L, Cohn J Roberts T, Ellman T, Bonner K, Rousseau C, Foundation MG, Garnett G, Foundation MG, Cambiano V, Ford D, Ford N, Vitoria M. Sustainable HIV Treatment In Africa Through Viral Load-Informed Differentiated Care. Nature 2016; 528(7580): S68-S76. https://doi.org/10.1038/nature16046

[22] Palmer A, Gabler K, Rachlis B, Ding E, Chia J, Bacani N, Bayoumi AM, Closson K, Klein M, Cooper C, Burchell A, Walmsley S, Kaida A, Hogg R. Viral Suppression And Viral Rebound Among Young Adults Living With HIV In Canada. Medicine 2018; 97(22): e10562. https://doi.org/10.1097/MD.0000000000010562

[23] Rachlis B, Cole DC, van Lettow M, Escobar M, Muula AS, Ahmad F, Orbinski J, Chan AK. Follow-Up Visit Patterns In An Antiretroviral Therapy (ART) Programme In Zomba, Malawi. PLoS ONE 2014; 9(7): e101875. https://doi.org/10.1371/journal.pone.0101875

[24] Asfaw A, Ali D, Eticha T, Alemayehu A, Alemayehu M. CD4 Cell Count Trends After Commencement Of Antiretroviral Therapy Among HIV- Infected Patients In Tigray , Northern Ethiopia : A Retrospective Cross-Sectional Study. PLoS ONE 2015; 652: 1-9. https://doi.org/10.1371/journal.pone.0122583

[25] Virally, Among, Patients, Suppressed Hiv-positive, Maskew M, Brennan AT, Westreich D. Gender Differences In Mortality And CD4 Count Response. Journal of Women's Health 2013; 22(2): 113-120. https://doi.org/10.1089/jwh.2012.3585

[26] Ingold H, Mwerinde O, Ross AL, Leach R, Corbett EL, Johnson CC, Ncube G, Nyirenda R, Baggaley RC. The Self-Testing AfRica (STAR) Initiative: Accelerating Global Access And Scale-Up Of HIV Self-Testing. Journal of the International AIDS Society 2019; 22: 94-100. https://doi.org/10.1002/jia2.25249

[27] Indravudh PP, Sibanda EL, Elbe M, Kumwenda MK, Ringwald B, Maringwa G, Simwinga M, Nyirenda LJ, Johnson CC, Hatzold K, Terris-Prestholt F, Taegtmeyer M. I Will Choose When To Test , Where I Want To Test: Investigating Young People ' S Preferences For HIV Self-Testing In Malawi And Zimbabwe. AIDS 2017; 31(Suppl 3): S203-S212. https://doi.org/10.1097/QAD.0000000000001516

[28] Mugurungi O. HIV Self-testing to address the testing gap in Zimbabwe. Health and Medicine 2015. URL https://www.slideshare.net/SlidesShare_Foxtrot/zimbabwe-hiv-self-testing-presentation [Accessed on 30 August 2019]

[29] Maskew M, Fox MP, Evans D, Govindasamy D, Jamieson L, Malete G, Mongwenyana C, Technau K. Insights Into Adherence Among A Cohort Of Adolescents Aged 12-20 Years In South Africa: Reported Barriers To Antiretroviral Treatment. AIDS Research and Treatment 2016; 2016: 1-13. https://doi.org/10.1155/2016/4161738

[30] Babo YD, Alemie GA, Fentaye FW. Predictors Of First-Line Antiretroviral Therapy Failure Amongst HIV-Infected Adult Clients At Woldia Hospital, Northeast Ethiopia. PLoS ONE 2017; 12(11): e0187694. https://doi.org/10.1371/journal.pone.0187694

[31] Dewing SF, Mathews C, Lurie M, Kagee A, Padayachee T, Lombard CJ, Health, Mental. Predictors Of Poor Adherence Among People On Antiretroviral Treatment In Cape Town, South Africa: A Case-Control Study. AIDS Care 2015; 27(3): 342-349. https://doi.org/10.1080/09540121.2014.994471

[32] Ryscavage PA, Anderson EJ, Sutton SH, Reddy S. Clinical Outcomes Of Adolescents And Young Adults In Adult HIV Care. Journal of Acquired Immne Deficiency Syndrome 2011; 58(2): 193-197. https://doi.org/10.1097/QAI.0B013E31822D7564

[33] Narayan KM, Venkat M, Paolo G, Anand NP, Kline LM, Harmston C, Iii RG, Vermund SH. Introduction HIV And Noncommunicable Disease Comorbidities In The Era Of Antiretroviral Therapy : A Vital Agenda For Research In Low- And Middle-Income Country Settings. Journal of Acquired Immne Deficiency Syndrome 2014; 67(1): S2-S7. https://doi.org/10.1097/QAI.0000000000000267

[34] Wabiri N, Shisana O, Zuma K, Freeman J. Assessing The Spatial Nonstationarity In Relationship Between Local Patterns Of HIV Infections And The Covariates In South Africa: A Geographically Weighted Regression Analysis. Spatial and Spatio-temporal Epidemiology 2016; 16: 88-99. https://doi.org/10.1016/j.sste.2015.12.003

[35] Rangarajan S, Donn JC, Giang LT, Bui DD, Hung N, Huu T, Plui B, Danh TT, Tran NBC, Nguyen DA, Hoang N, Bao T, Doan VTN, Nguyen NQ, Pham VP, Dao DG, Chen M, Zeng Y, Tieu TTV, Tran MH, Le TH, Hoang XC, West G. Factors Associated With HIV Viral Load Suppression On Antiretroviral Therapy In Vietnam. Journal of Virus Eradication 2016; 2(2): 94-101.

[36] Bock P, Gunst C, Maschilla L, Holtman R, Grobbelaar N, Wademan D, Dunbar R, Fatti G, Kruger J, Ford N, Hoddinott G, Meehan S-A. Retention In Care And Factors Critical For Effectively Implementing Antiretroviral Adherence Clubs In A Rural District In South Africa. Journal of the International AIDS Society 2019; 22: e25396. https://doi.org/10.1002/jia2.25396

[37] Ferrand RA, Simms V, Dauya E, Bandason T, Mchugh G, Mujuru H, Chonzi P, Busza J, Kranzer K, Munyati S, Weiss HA, Hayes RJ. The Effect Of Community-Based Support For Caregivers On The Risk Of Virological Failure In Children And Adolescents With HIV In Harare, Zimbabwe (ZENITH): An Open-Label, Randomised Controlled Trial. The Lancet Child and Adolescent Health 2017; 1(3): 175-183. https://doi.org/10.1016/S2352-4642(17)30051-2

[38] Maponga BA, Chirundu D, Gombe NT, Tshimanga M, Bangure D, Takundwa L. Delayed Initiation Of Anti-Retroviral Therapy In TB/HIV Co-Infected Patients, Sanyati District, Zimbabwe, 2011-2012. Pan African Medical Journal 2015; 21: 2011-2012. https://doi.org/10.11604/pamj.2015.21.28.5195

[39] Nyika H, Mugurungi O, Shambira G, Gombe NT, Bangure D, Mungati M, Tshimanga M. Factors Associated With Late Presentation For HIV / AIDS Care In Harare City , Zimbabwe, 2015. BMC Public Health 2016; 16(369): 1-7. https://doi.org/10.1186/s12889-016-3044-7

[40] Clements ACA, Lwambo NJS, Blair L, Nyandindi U, Kaatano G, Kinung S, Webster JP, Fenwick A. Bayesian Spatial Analysis And Disease Mapping: Tools To Enhance Planning And Implementation Of A Schistosomiasis Control Programme In Tanzania. Tropical Medicine & International Health 2006; 11(4): 490-503. https://doi.org/10.1111/j.1365-3156.2006.01594.x

[41] Chitunhu S, Musenge E. Spatial And Spatio-Temporal Epidemiology Spatial And Socio-Economic Effects On Malaria Morbidity In Children Under 5 Years In Malawi In 2012. Spatial and Spatio-temporal Epidemiology 2016; 16: 21-33. https://doi.org/10.1016/j.sste.2015.11.001

[42] Kapadia SN, Grant RR, German SB, Singh B, Davidow AL, Swaminathan S, Hodder S. HIV Virologic Response Better With Single-Tablet Once Daily Regimens Compared To Multiple-Tablet Daily Regimens. SAGE Open Medicine 2018; 6: 1-8. https://doi.org/10.1177/2050312118816919

[43] Truong WR, Schafer JJ, Short WR. Once-Daily, Single-Tablet Regimens For The Treatment Of HIV-1 Infection. P & T: A peer-reviewed Journal for Formulary Management 2015; 40(1): 44-55.

[44] Nicholas S, Poulet E, Wolters L, Wapling J, Rakesh A, Amoros I, Szumilin E, Gueguen M, Schramm B. Point-Of-Care Viral Load Monitoring: Outcomes From A Decentralized HIV Programme In Malawi. Journal of the International AIDS Society 2019; 22(8): 1-9. https://doi.org/10.1002/jia2.25387

[45] World Health Organization. HIV Treatment and Care What's new in Treatment Monitoring: Viral load and CD4 Testing. WHO 2017. URL https://www.who.int/hiv/pub/arv/treatment-monitoring-info-2017/en/ [Accessed 26 November 2018].

[46] Ministry of Health and Child Care (MOHCC), Zimbabwe. Zimbabwe Population-Based HIV Impact Assessment (ZIMPHIA) 2015-2016: First Report. MOHCC Harare 2017. URL https://phia.icap.columbia.edu/wp-content/uploads/2017/11/ZIMPHIA_First_Report_FINAL.pdf [Accessed on 7 December 2019]

[47] Anderson C, Lee D, Dean N. Bayesian Cluster Detection Via Adjacency Modelling. Spatial and Spatio-temporal Epidemiology 2016; 16: 11-20. https://doi.org/10.1016/j.sste.2015.11.005

Received on 25-11-2019 Accepted on 12-12-2019 Published on 20-12-2019

https://doi.org/10.6000/1929-6029.2019.08.13